Design and Implementation of Single-Carrier MIMO Transmission with Frequency Domain Equalization*

Liang Liu[a], Yong Liang Guan[b], Yanzhong Zhang[a], Dingrong Shao[a]

[a] Beihang University, Beijing, China

[b] Nanyang Technological University, Singapore

Abstract: A multiple-input multiple-output (MIMO) single-carrier frequency domain equalization (SC-FDE) testbed which can emulate a practical broadband system is described. A scheme combining space-time transmit diversity with SC-FDE was implemented and evaluated on the testbed. After the hardware configuration, software algorithms incorporating the space-time block coding and decoding, synchronization, channel estimation and frequency domain equalization are explained, followed by some field measurements which validating our design and implementation. It is showed that this software reconfigurable testbed is flexible and convenient to evaluate different system performance in kinds of wireless environments.

Keywords: single-carrier frequency domain equalization; multiple-input multiple-output; testbed; space-time block code

1. Introduction

Wireless broadband communication systems are characterized by severe time-dispersive channels. To deal with the detrimental effects of multipath fading, two block transmission schemes can be adopted: single-carrier modulation with frequency domain equalization (SC-FDE) and orthogonal frequency division multiplexing (OFDM)[1]. Although there are already tremendous applications of OFDM which range from DAB and DVB standards to wireless LAN standards, SC-FDE, which enjoys lower peak-to-average transmit power ratio and less sensitivity to carrier frequency offset than that of OFDM, has been elected as a promising technique for future broadband wireless networks[2-4].

On the other hand, digital communication using MIMO (multiple-input multiple-output), sometimes called a volume-to-volume wireless link, has recently emerged as one of the most significant technical breakthroughs in modern communications[5]. MIMO technology promises high data rate wireless communications and/or the potentiality of exploiting spatial transmit and receive diversity schemes[6]. Therefore, combining MIMO with SC-FDE has been identified as one key

* Published in the 5th Intl. Conf. con Computer Science & Education, Aug. 2010: 56-60.

Y. Zhang, *Footprints in Cambridge and Aviation Industries of China*,
https://doi.org/10.1007/978-981-16-3176-4_21

technique for supporting high data rates over frequency-selective fading channels. It has been shown in [7] that SC-FDE with Alamouti's space-time block codes (STBC) leads to significantly improved performance owing to the joint exploitation of spatial-frequency diversity in a rich scattering environment.

Although many papers have examined the remarkable performance of MIMO SC-FDE systems, most of their works still focus on the theoretical researches or computer simulations. In order to validate these theoretical conclusions, a testbed system, is emergent and essential to run in a real-world wireless environment and consider the presence of all analog hardware impairments. There have been a flourishing work on the evaluation MIMO-OFDM system through testbeds[8, 9]. However, to the best of the author's knowledge, there are few works reported the performance evaluation of MIMO SC-FDE under real-time or non-real-time testbed, which motivates us to address this issue.

In this paper, a MIMO SC-FDE testbed with WiMAX-like architecture is described, which is used to study practical issues in both RF and baseband models. Then a specific space-time coded SC-FDE was implemented on this testbed. It is worth emphasizing that this testbed is software reconfigurable and flexible to alter the system parameters such as carrier frequency, bandwidth, frame format, and transmission/reception antennas structures.

The remainder of the paper is organized as follows: In Section 2, the system model and architecture are described. The main baseband algorithms are introduced in Section 3. In Section 4, the implementation and field measurement results are given. Finally future relevant research works based on the MIMO SC-FDE testbed are introduced.

Notation: We denote matrices by bold uppercase letters and column vectors by bold lowercase letters; $(\cdot)_N$, $(\cdot)^*$, $(\cdot)^H$, and $(\cdot)^{-1}$ denote modulo-W operation, conjugate, conjugate transpose, and inverse, respectively; $D(h)$ represents a diagonal matrix with the diagonal coefficients from the vector h; The mark "$\sim$" on top of a vector denotes the frequency domain representation of the time domain signal.

2. System Model and Architecture

In this section, we introduce the configuration of a specific space-time coded SC-FDE system based on a software-defined radio (SDR) testbed. The testbed consists of a transmitter and a receiver, each of which can be divided into hardware and software components. The National Instrument (NI) equipments construct the basic hardware architecture of the testbed. At the same time, the NI LabVIEW, embedding MATLAB, is programmed to control the hardware and perform the baseband signal generation, modulation, demodulation, equalization and decoding. All the baseband processing algorithms are achieved in the MATLAB environment.

The overall block diagram of the proposed space-time coded SC-FDE system is illustrated in Fig. 1. At the transmitter, the randomly generated bits are modulated according to MPSK or MQAM format, and subsequently space-time coded by Alamouti code[10]. Then the modulated signals are preceded with two preambles to constitute one frame and pushed into the LabVIEW to

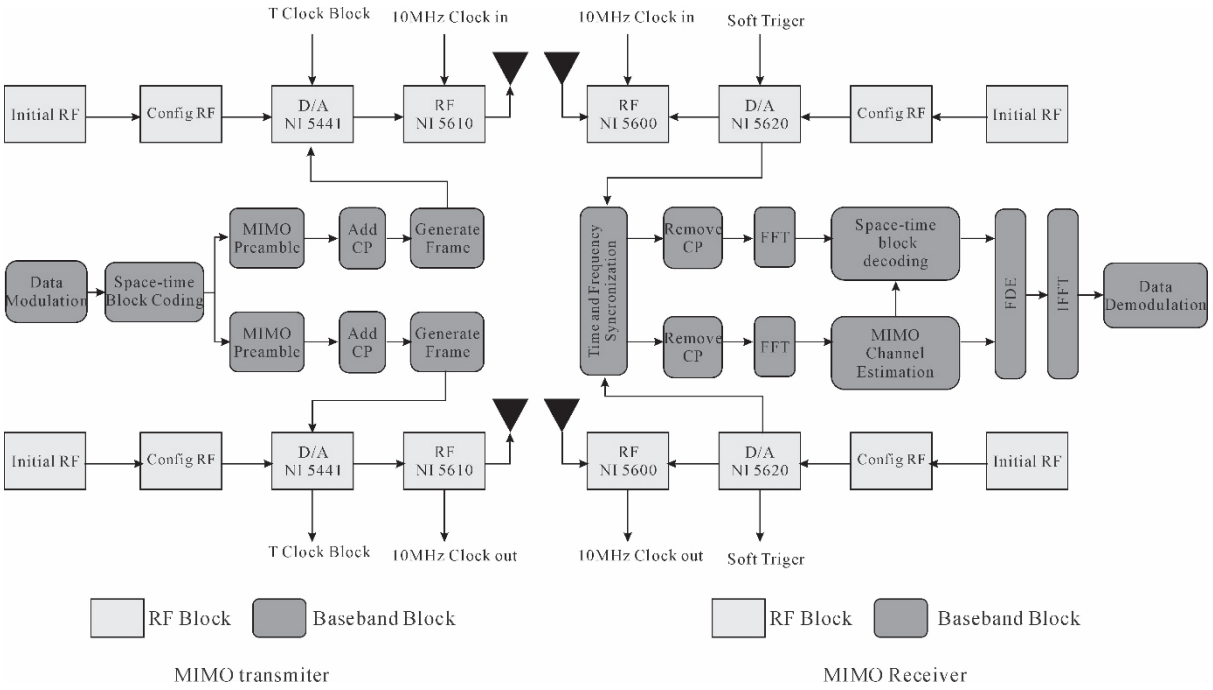

Fig. 1 Block diagram of the 2×2 MIMO SC-FDE testbed

drive the NI hardware to generate the analog waveform. At the receiver, the RF signals are received and downconverted by the RF hardware which are controlled by LabVIEW. The sampled data are then sent into MATLAB for baseband signal processing, including synchronization, fast Fourier transform (FFT), space-time decoding, FDE and inverse FFT (IFFT).

3. Algorithms of the Transceiver Functional Block

For the MIMO SC-FDE testbed, the RF blocks such as D/A, A/D and frequency converters are relatively mature. Thus in this section, we focus on the baseband signal processing such as frame generation, synchronization, channel estimation, space-time block decoding and FDE.

3.1 Frame Structure

The MIMO SC-FDE testbed supports a frame-by-frame transmission. Each frame starts with two preambles: a short preamble and a long preamble, where the short preamble is used for synchronization while the long preamble is constructed for the channel estimation. The preambles are followed by payload SC-FDE symbols. In our testbed, we set the payload length to be 4 to accommodate the WiMAX standard (termed it as WiMAX-like architecture). For 2×2 MIMO transmission case, the frame structure is shown in Fig. 2.

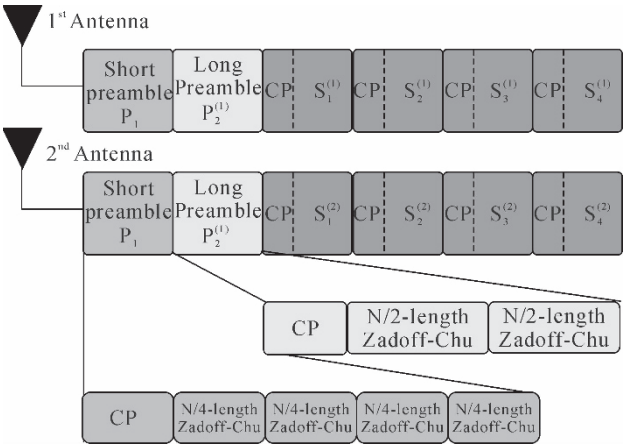

Fig. 2 Frame structure of the proposed 2×2 space-time coded SC-FDE system

It can be seen from Fig. 2 that the concatenated two preambles are structured as two consecutive SC-FDE blocks. The first SC-FDE block consists of four repetition of $N/4$-length Zadoff-Chu sequences[11], where N represents the number of modulated symbols in each SC-FDE block. A cyclic prefix (CP) which is a repetition of the last $N_g = N/4$ symbols in a SC-FDE block, is inserted at the beginning of each block. The second SC-FDE block are constructed by two identical $N/2$-length Zadoff-Chu sequences, preceded by CP. It should be noted that the preamble shall be transmitted from both transmit antennas simultaneously. The short preamble is set to be the same for both of the two antennas while the long preamble be different to guarantee that the channel estimation at each receiver antenna can be performed without interference from the other antenna. Specifically in the frequency domain, the long preamble transmitted from the first antenna uses only the even subcarriers, and the second antenna uses odd subcarriers.

Denote the nth modulated symbol of the k th SC-FDE block from antenna j by $s_k^{(j)}(n)$. In order to employ the Alamouti's STBC to achieve spatial diversity, the signals need to be coded as follows (see Fig. 2)

$$\begin{cases} s_{k+1}^{(1)}(n) = -\{s_k^{(2)}((-n)_N)\}^* \\ s_{k+1}^{(2)}(n) = \{s_k^{(1)}((-n)_N)\}^* \end{cases} \quad k = 1 \text{ or } 3, n = 0, 1, \cdots, N-1 \tag{1}$$

Thus it satisfies the Alamouti architecture in the frequency domain as

$$\begin{cases} \tilde{s}_{k+1}^{(1)}(m) = -\{\tilde{s}_k^{(2)}(m)\}^* \\ \tilde{s}_{k+1}^{(2)}(m) = \{\tilde{s}_k^{(1)}(m)\}^* \end{cases} \quad k = 1 \text{ or } 3, m = 0, 1, \cdots, N-1 \tag{2}$$

3.2 Time and Frequency Synchronization

It is well known that residual time and frequency offset due to non-ideal synchronization result in significant performance degradation, especially for block-based system. Hence, robust time and frequency synchronization is expected to be performed at the receiver.

1) Time synchronization: In order to accurately find the starting point of the frame in the presence of frequency offset and multipath, we resort to a preamble-aided cross-correlation method

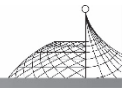

given in (3)

$$C(m) = \frac{\left| \sum_{k=0}^{N/4-1} r(m+k)\beta_1^*(k) \right|^2}{\sum_{k=0}^{N/4-1} |r(m+k)|^2} \quad m = 1,2,\cdots,N_{\text{samp}} \tag{3}$$

where $\beta_1(k)$ is the Zadoff-Chu training sequence with the length $N/4$ of the short preamble. $r(m+k)$ represents the samples of the received signal whose length is N_{samp}. Having obtained the cross-correlation $C(m)$, we may further calculate its partial auto-correlation $PA(m)$ as

$$PA(m) = \sum_{i=0}^{4} C(m+i \cdot N/4) \quad m = 1,2,\cdots,N_{\text{samp}}-5 \tag{4}$$

Relying on (4), the starting point of the frame could be located by configuring adaptive threshold and searching the position of the pulse peak.

2) Frequency synchronization: Frequency synchronization can be divided into two steps: frequency offset estimation and compensation. After the frame detection, the fractional frequency offset $\hat{\varepsilon}_{\text{FFO}}$ can be readily estimated by exploiting the repeated feature of the short preamble

$$\hat{\varepsilon}_{\text{FFO}} = \frac{1}{\pi}\arg\{\sum_{m=0}^{L-1} r(m)r^*(m+N/2)\} \tag{5}$$

where L is set to $3N/4$. The maximal FFO that can be estimated is $\max\{\hat{\varepsilon}_{\text{FFO}}\} = \pm 1$ (normalized by virtual subcarrier spacing). Then the received preambles are compensated using the estimated $\hat{\varepsilon}_{\text{FFO}}$,

$$\hat{r}(n) = r(n)\exp\{-j2\pi\hat{\varepsilon}_{\text{FFO}}\frac{n}{N}\} \tag{6}$$

Once the fractional frequency offset is compensated, the FFT of the preambles will be circularly shifted by an even number of frequency subcarriers. The remaining integer frequency offset $\hat{\varepsilon}_{\text{IFO}}$ can be easily estimated by introducing the algorithms developed in [12]. Then the frequency synchronization of the payload part can be achieved using (6) by substituting $\hat{\varepsilon}_{\text{FFO}}$ with $\hat{\varepsilon}_{\text{FFO}} + \hat{\varepsilon}_{\text{IFO}}$.

3.3 Channel Estimation

As indicated in Section 1, we utilize the long preamble to perform channel estimation. In order to maintain orthogonality between two antennas, antenna 1 uses odd virtual subcarriers, and antenna 2 uses even virtual subcarriers to transmit training symbols.

Define $r_k^{(j)}$ denotes the received vector from the jth antenna of the kth SC-FDE block. Thus the received long preamble signal may be illustrated as

$$r_k^{(j)} = H_{j,1}p_2^{(1)} + H_{j,2}p_2^{(2)} + n^{(j)} \tag{7}$$

where $H_{j,t}$ represents the equivalent circulant channel matrix from transmit antenna t to the receive antenna j. Relying on the property that a circulant matrix can be decomposed into a diagonal matrix and applying FFT to $r_k^{(j)}$, we get

$$\tilde{r}_k^{(j)} = D(\tilde{h}_{j,1})\tilde{p}_2^{(1)} + D(h_{j,2})\tilde{p}_2^{(2)} + \tilde{n}^{(j)} \tag{8}$$

where $\tilde{h}_{j,1}$ and $\tilde{h}_{j,2}$ represent the channel frequency responses.

Estimation of the channel at the virtual subcarrier points can be done on the basis of least square (LS) and minimum mean square error (MMSE) criteria. Although MMSE performs better than LS, it needs knowledge of the channel statistics and the operating SNR. Thus we choose LS to tradeoff

between implementation feasibility and system performance. The channel frequency responses $\tilde{h}_{j,t}(n), j=1,2$ are obtained by dividing $\tilde{r}_k^{(j)}(n)$ by the training symbols $\tilde{p}_2(n)$. In MIMO case, there have only half subcarriers can be used for each antenna. So linear interpolation is performed to obtain the channel frequency response $\tilde{h}_{j,t}$ for all the subcarriers corresponding to each transmission-reception antenna set.

3.4 Space-Time Decoding and FDE

Similar as (8), the received frequency domain payload signals are given by

$$\begin{cases} \tilde{r}_k^{(j)} = D(\tilde{h}_{j,1})\tilde{s}_k + D(\tilde{h}_{j,2})\tilde{s}_{k+1} + \tilde{n}_k^{(j)} \\ \tilde{r}_{k+1}^{(j)} = D(\tilde{h}_{j,1})(-\tilde{s}_k^*) + D(\tilde{h}_{j,2})\tilde{s}_{k+1}^* + \tilde{n}_{k+1}^{(j)} \end{cases} \quad j=1,2 \tag{9}$$

After some manipulations on (9), we get

$$\tilde{r}^{(j)} = \begin{bmatrix} \tilde{r}_k^{(j)} \\ (\tilde{r}_{k+1}^{(j)})^* \end{bmatrix} = \begin{bmatrix} D(\tilde{h}_{j,1}) & D(\tilde{h}_{j,2}) \\ -D^*(\tilde{h}_{j,2}) & D^*(\tilde{h}_{j,1}) \end{bmatrix} \begin{bmatrix} \tilde{s}_k \\ \tilde{s}_{k+1} \end{bmatrix} + \begin{bmatrix} \tilde{n}_k^{(j)} \\ (\tilde{n}_{k+1}^{(j)})^* \end{bmatrix} \tag{10}$$

Combining $\tilde{r}^{(1)}$ and $\tilde{r}^{(2)}$ in (10), we get

$$\tilde{r} = \begin{bmatrix} \tilde{r}_k^{(1)} \\ (\tilde{r}_{k+1}^{(1)})^* \\ \tilde{r}_k^{(2)} \\ (\tilde{r}_{k+1}^{(2)})^* \end{bmatrix} = \underbrace{\begin{bmatrix} D(\tilde{h}_{1,1}) & D(\tilde{h}_{1,2}) \\ -D^*(\tilde{h}_{1,2}) & D^*(\tilde{h}_{1,1}) \\ D(\tilde{h}_{2,1}) & D(\tilde{h}_{2,2}) \\ -D^*(\tilde{h}_{2,2}) & D^*(\tilde{h}_{2,1}) \end{bmatrix}}_{\Theta} \begin{bmatrix} \tilde{s}_k \\ \tilde{s}_{k+1} \end{bmatrix} + \tilde{n} \tag{11}$$

Since Θ is an orthogonal matrix, we can multiply both sides of (11) by Θ^H to decouple the two signals $\tilde{s}_k$ and $\tilde{s}_{k+1}$ resulting in

$$\hat{r} = \Theta^H \tilde{r} = \begin{bmatrix} \tilde{\Theta} & 0 \\ 0 & \tilde{\Theta} \end{bmatrix} \begin{bmatrix} \tilde{s}_k \\ \tilde{s}_{k+1} \end{bmatrix} + \hat{n} \tag{12}$$

where $\tilde{\Theta} = |D(\tilde{h}_{1,1})|^2 + |D(\tilde{h}_{1,1})|^2 + |D(\tilde{h}_{1,1})|^2 + |D(\tilde{h}_{1,1})|^2$ is an $N \times N$ diagonal matrix. Note that (12) signifies that the order-four spatial diversity gain can be achieved by this scheme. Applying the same FDE method as in SISO case, the frequency domain equalization matrix G maybe expressed as

$$G = \Theta^H (\Theta\Theta^H + \rho/\mathrm{SNR})^{-1} \tag{13}$$

where weight $\rho=1$ denotes MMSE-FDE, while $\rho=0$ represents the ZF-FDE. Then the estimated signal $\tilde{s}_k$ and $\tilde{s}_{k+1}$ could be easily obtained via IFFT processing.

4. Implementation and Field Measurements

One photo of our implemented testbed is given in Fig. 3. In this section, we present some of the measurement results to validate the system design and baseband signal processing algorithms. The

system parameters are listed in Table 1. It is worth mentioning that the developed testbed is software reconfigurable, so all the parameters can be altered conveniently.

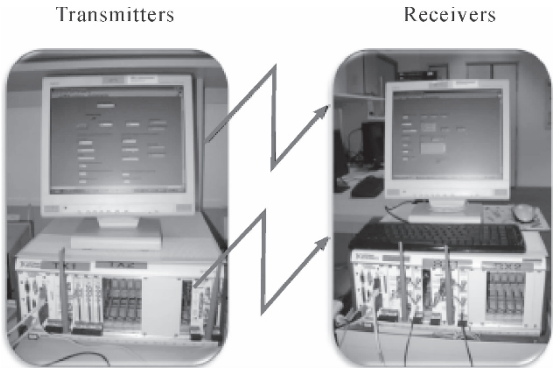

Fig. 3 MIMO SC-FDE testbed for fireld measurements

Table 1 System parameters

Carrier frequency	2.38 GHz
Bandwidth	8 MHz
FFT size	$N=256$
Cyclic Prefix ratio	$N_g/N=1/4$
SC-FDE block duration	32 μs+8 μs(Guard Interval)
Modulation	QPSK
Frame structure	2 preambles+4 data symbols
Frequency domain equalization	ZF-FDE

Before performing field trials, the synchronization of two hardware equipments has to be considered to accommodate the multiple antennas' transmission (see Fig. 1). Firstly, we need to synchronize the RF local oscillators (LO). At the TX, the first NI-5610 generates a 10 MHz clock signal and feed this clock signal to the second NI-5610 to achieve clock synchronization for the LO. At the RX, the first NI-5610 feeds its 10 MHz clock signal to the PXI chassis backplane and the second NI-5600 is then driven by the backplane clock. Next, the two sets of NI-5441 acting as D/A (NI-5620 acting as A/D) also have to be synchronized. At the TX, this is realized by the T-clock block. However at the RX, the NI hardware does not support the T-clock block and thus we resort to using a software trigger to achieve synchronization between the two NI-5620.

In order to validate the design, we perform the field measurements in the non-line-of-sight (NLOS) environment.

Fig. 4 shows the time synchronization results. It can be seen that the correlation calculation is performed in the first 5000 points (i.e. $N_{\text{samp}}=5000$). Since each frame has $320*6=1920$ points, the frame detection can be guaranteed within the 5000 samples. The top figure shows the cross-correlation results $C(m)$, where five peaks could be detected due to the five repeated parts in the short preamble. The bottom figure plots the partial auto-correlation of $C(m)$ from which the peak

corresponding to the starting point of a frame could be obtained.

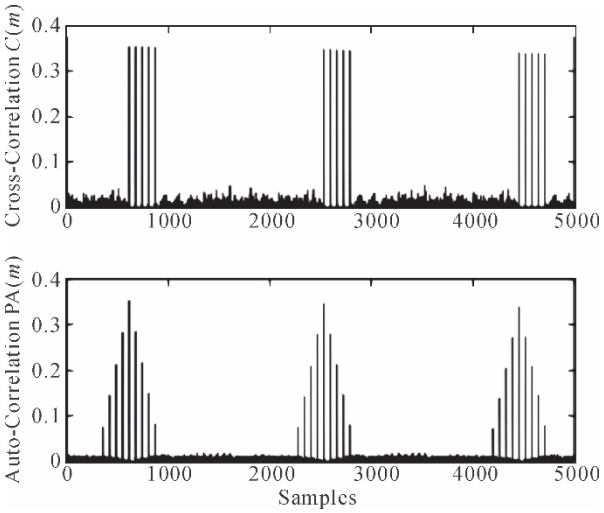

Fig. 4 Synchronization results using the short preamble

Fig. 5 shows the constellations and channel frequency response measurement results at the received RF power-40 dBm. The channel frequency response are obtained by averaging 20 frames on all 256 subcarriers. It can be observed that for different TX-RX antennas links, the channel fadings are different for each other. Some links are flat-fading like channel like Fig. 5 (f) and (g), while others may suffer from frequency-selective fading, like Fig. 5 (e) and (h). However, in the presence of fading, the detected signals are still within the correction region as shown in Fig. (a)(b)(c)(d), owing to the spatial-frequency diversity provided by space-time block codes and single-carrier frequency domain equalization. This measurement results validate our system design and implementation.

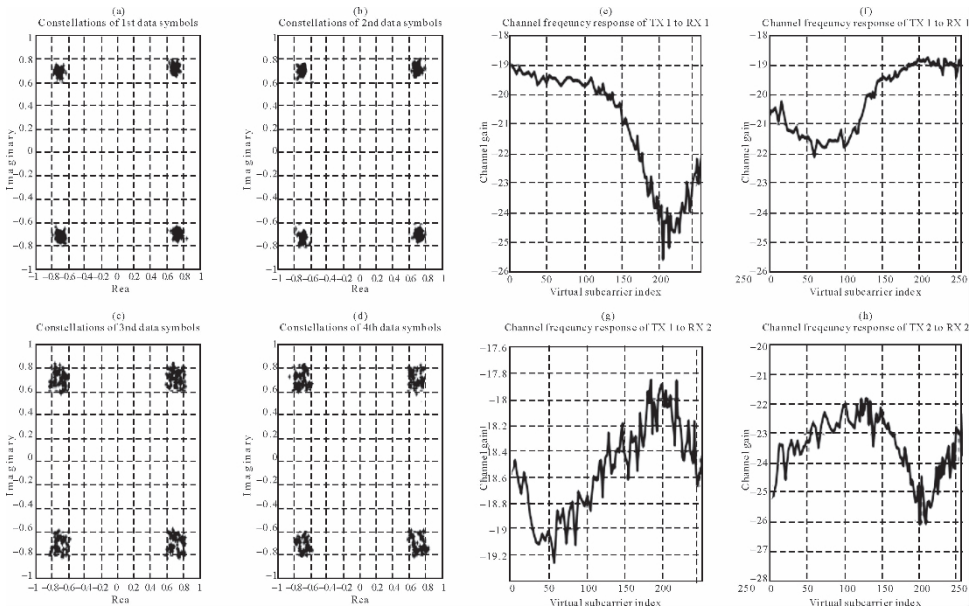

Fig. 5 Constellations and channel frequency response at received power-40 dBm over a NLOS environment

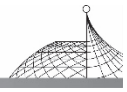

5. Conclusion

In this paper, we introduce a software defined MIMO SC-FDE testbed, based on which a specific space-time coded SC-FDE system was implemented. The developed testbed has some advantages. Firstly, it is software reconfigurable, which means we can easily change the kernel of the experiment system. Baseband processing are all achieved in the MATLAB environment. So we can just alter the MATLAB function to alter the system structure, such as frame fragment, modulation and coding methods, antenna selection, etc. Secondly, the testbed has a tunable RF front-end. Using NI equipments, the RF parameters including carrier frequency and bandwidth can be adjusted optionally.

However, only a preliminary work has been done on the testbed, our future work will focus on the design of SC-FDE system with spatial multiplexing and MIMO SC-FDE with multi-access (i. e. MIMO SC-FDMA)[13]. At the same time, any robust algorithms, such as channel estimation, frequency domain equalization over time-selective fading channels can be developed on this testbed.

Acknowledgment

The authors would like to thank Dr. D. W. Liu and Mr. Y. X. Yan from Positioning and Wireless Technology Center, Nanyang Technological University, for their technical reports and useful discussions. The first author also acknowledges the Chinese Scholarship Council (CSC) for providing scholarship to support this research.

References

[1] N. Benvenuto and S. Tomasin, "On the Comparison Between OFDM and Single Carrier Modulation With a DFE Using a Frequency-Domain Feedforward Filter.", IEEE Trans. Commun., vol. 50, no. 6, pp. 947-955, June 2002.

[2] H. Sari, G. Karam, and I. Jeanclaude, "Transmission Techniques for Digital Terrestrial TV Broadcasting." IEEE Commun. Mag., vol. 33, no. 2, pp. 100-109, Feb. 1995.

[3] D. Falconer, S. L. Ariyavisitakul, A. Benyamin-Seeyar, and B. Eidson, "Frequency domain equalization for single-carrier broadband wireless systems." IEEE Commun. Mag., vol. 40, no. 4, pp. 58-66, Apr. 2002.

[4] N. Benvenuto, R. Dinis, D. Falconer, and S. Tomasin, "Single carrier modulation with nonlinear frequency domain equalization: an idea whose time has come-again." IEEE Proceeding, vol. 98, no. 1, pp. 69-96, Jan. 2010.

[5] D. Gesbert, M. Shafi, D. S. Shiu, et al., "From theory to practice: An overview of MIMO space-time coded wireless systems." IEEE J. Select. Areas Commun., vol. 21, no. 3, pp. 281-302, Apr. 2003.

[6] A. J. Paulraj, D. Gore, R. U. Nabar, H. Btilcskei, "An Overview of MIMO Communications: A

Key to Gigabit Wireless." IEEE Proceeding, vol. 92, no. 2, pp. 198-218, Feb. 2004.

[7] S. Zhou, G. B. Giannakis, "Single-Carrier SpaceCTime Block-Coded Transmissions Over Frequency-Selective Fading Channels." IEEE Trans. Inform. Theory, vol. 49, no. 1, pp. 164-179, Jan. 2003.

[8] A. V. Zelst and T. C. W. Schenk, "Implementation of a MIMO-OFDM based wireless LAN system." IEEE Trans. Signal Processing, vol. 52, no. 2, Feb. 2004.

[9] R. M. Rao, S. Lang, and B. Daneshrad, "Field measurements with a 5.25 GHz broadband MIMO-OFDM communication system." IEEE Trans. Wireless Commun., vol. 6, no. 8, pp 2848-2858, Aug. 2007.

[10] S. M. Alamouti, "A simple transmit diversity technique for wireless communications." IEEE J. Select. Areas Commun., vol. 16, no. 8, pp. 1451-1458, Apr. 1998.

[11] D. C. Chu, "Polyphase codes with good periodic correlation properties." IEEE Trans. Inform. Theory, vol. 18, pp. 531-532, Jan. 1992.

[12] Y. Yan, Y. Gong, Y. L. Guan et al., "Joint timing and frequency synchronization for IEEE 802.16 OFDM system." IEEE WiMAX Symposium, Mar. 2007, pp. 27-31.

[13] Z. H. Lin, P. Xiao, B. Vucetic, et al., "Analysis of receiver algorithms for LTE SC-FDMA based uplink MIMO systems." IEEE Trans. Wireless Commun., vol. 9, no. 1, pp. 61-65, Jan. 2010.